ChemComm

COMMUNICATION

View Article Online
View Journal | View Issue

Cite this: *Chem. Commun.*, 2021, **57**, 343

Received 1st November 2020,
Accepted 26th November 2020

DOI: 10.1039/d0cc07226e

rsc.li/chemcomm

Disaggregation of a sumanene-containing fluorescent probe towards highly sensitive and specific detection of caesium cations†

Artur Kasprzak *[a] and Hidehiro Sakurai [b]

A sumanene derivative functionalized with triphenylbenzene units was found to exhibit aggregation-induced emission enhancement (AIEE). A disaggregation process after the addition of caesium cations (Cs^+) was observed. This feature was employed for the design of the first sumanene-containing disaggregation-based fluorescent probe for specific, efficient and fast Cs^+ recognition.

Sumanene, a fullerene subunit, is an organic compound belonging to the class of so-called *buckybowls*.[1–3] Over the years, derivatization of sumanene aimed at creating novel functional organic molecules has been investigated.[4–7] Due to the presence of curvature in their structures, the properties and functions of bowl-shaped sumanene derivatives are different from those of their planar aromatic congeners. The formation of a non-planar, two-dimensional framework with hydrogen-bonded networks composed of a hexa-carboxylated sumanene derivative in contrast to the planar hexagonal networks of triphenylene analogues is a typical example.[8]

It is worth noting that functionalized sumanenes have become molecules of interest in coordination chemistry. For example, hexapyridylsumanenes have recently been applied to the construction of organometallic capsules.[9] Changing the metal ion from zinc to cadmium enabled the arrangement of the cage to be tuned from belt-like to spherical. In another report, solid-state self-assembly studies with sumanenylferrocenes revealed unique packing motifs for these derivatives.[10] The research work has also covered the use of native sumanene as a ligand in organometallic complexes. Both convex- and concave-oriented sumanene complexes were synthesized, *e.g.* the convex-bound hafnocene complex[11] or concave-bound iron[12] and ruthenium[13] complexes. Interestingly, in 2017, the isolation of a sandwich complex composed of two sumanenyl monoanions and a caesium cation (Cs^+) was reported.[14] Sumanenyl monoanions were synthesized by the treatment of sumanene with sodium. This process resulted in a solvent-separated ion pair. Cs^+ encapsulation by two sumanenyl monoanions was driven by the perfect match between the Cs^+ ion and the concave site of sumanene.

Recently, we reported that sumanene is also able to interact with Cs^+ in its neutral state.[15,16] This interaction is driven by the site-selective cation–π-interaction that occurs following inclusion in the concave site of sumanene.[17–19] We have demonstrated that the Cs^+ recognition process is specific and effective for the ferrocene-functionalized sumanenes. Inspired by these findings, we further studied the application of sumanene-tethered molecules towards the rapid recognition of Cs^+. Herein, we report the synthesis of a novel sumanene derivative bearing three triphenylbenzene units – a yellow-light emitting molecule exhibiting an aggregation-induced emission enhancement (AIEE) effect. Additionally, we report the application of this compound as a remarkably specific, selective, effective and sensitive turn-off fluorescent probe for Cs^+ detection. It is worth noting that Cs^+ detection is of greatest importance from the environmental viewpoint, since significant amounts of caesium have been detected in many radiated, post-disaster areas (such as after the nuclear plant accident in Fukushima-Daiichi in 2011).[20–22]

The synthetic pathway to obtain derivative **5** is shown in Scheme 1. In general, the target compound was obtained in good yields following the reported procedure,[23] using sumanene (**4**) and 1-(4-formylphenyl)-3,5-diphenylbenzene (**3**) as reactants. Compound **3** was prepared from 3,5-diphenylbromobenzene (**1**) and 4-formylphenylboronic acid (**2**) using a Suzuki–Miyaura cross-coupling reaction. Full experimental details can be found in Section S1 of the ESI.† The formation of a pure compound was confirmed using NMR spectroscopy, high-resolution mass spectrometry (HRMS) and elemental analysis (see the ESI,† for the compound characterization data). Similar to other sumanene derivatives prepared using the method described herein,[16,23] the NMR analyses revealed the formation of diastereoisomers (unsymmetrical and C_3 symmetric).

[a] *Faculty of Chemistry, Warsaw University of Technology, Noakowskiego Str. 3, Warsaw 00-664, Poland. E-mail: akasprzak@ch.pw.edu.pl*

[b] *Division of Applied Chemistry, Graduate School of Engineering, Osaka University, 2-1 Yamadaoka, Suita, Osaka 565-0871, Japan*

† Electronic supplementary information (ESI) available: Experimental details, NMR spectra, emission spectra and related data, and DLS data. See DOI: 10.1039/d0cc07226e

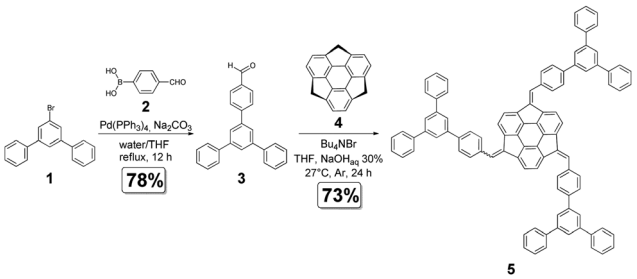

Scheme 1 Synthesis path to obtain the target compound (**5**).

Compound **5** exhibited yellow light emission in solution (Fig. 1a and b). Absorption spectra of **5** were measured in the following solvents: dichloromethane (DCM), chloroform and acetonitrile (ACN) (Fig. 1c). In the solvents tested, **5** showed several absorption maxima (λ_{abs}), namely 253–260 nm, 365–367 nm and 478 nm. No significant solvent-dependent shifts, either hypsochromic or bathochromic, were found between the solvents. The emission spectra of **5** were measured in $CHCl_3$ using different excitation wavelengths (λ_{ex}; Fig. 1d). Compound **5** exhibited an emission maximum (λ_{em}) at 548 nm. The highest emission intensity was found for λ_{ex} = 360 nm. The emission intensity was significantly reduced at higher concentrations (Fig. S5, ESI†), and this could be ascribed to the concentration quenching effect. The emission spectrum of **5** in the solid state was similar to that in $CHCl_3$ solution (λ_{ex} = 360 nm; see the orange dotted line in Fig. 1d). Only a small red shift of *ca.* 10–12 nm was found for the powdered sample.

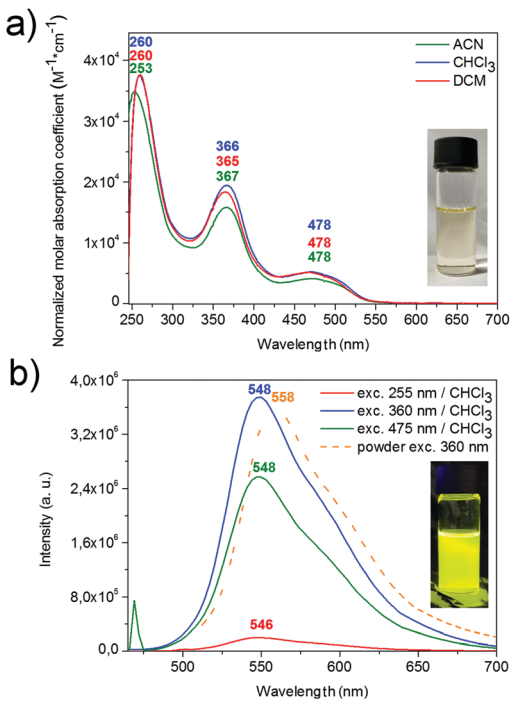

Fig. 1 (a) UV-Vis spectra of **5**; (b) emission spectra of **5** in $CHCl_3$ solution and in the solid state (powdered sample). The colours for the $CHCl_3$ solution of **5** (a) and using an excitation of 365 nm (b) are shown in the insets. The concentration of the samples is 2×10^{-5} M.

Next, emission spectra of **5** were measured in different mixtures of $CHCl_3$–hexane or $CHCl_3$–CH_3OH where the volume fraction of poor solvent (hexane or CH_3OH) was 0–95 vol%. This experiment was performed to check whether **5** shows the aggregation-induced emission enhancement (AIEE) effect.[24–26] The results for the $CHCl_3$–CH_3OH mixtures are presented in Fig. 2, whilst the data for the $CHCl_3$–hexane mixtures are presented in Fig. S6 of the ESI.† In both cases, the emission intensity at 548 nm did not change much up to 70 vol% of poor solvent. After this point, a continuous and significant increase in the emission intensity was observed as the ratio of poor solvent increased. This emission intensity change was also followed by an increase in emission quantum yields from 40–42% for 0 vol% of poor solvent to 89–92% for 95 vol% of poor solvent (see the full data in Section S4 of the ESI†). These trends clearly indicate that **5** is AIEE-active. Time-dependent studies for aggregated **5** revealed that the emission intensity increased significantly up to 7 minutes after the sample preparation and it then reached a constant value up to 24 hours (Fig. S7, ESI†). To further study the aggregate formation, dynamic light scattering (DLS) experiments were performed. For the samples with 95 vol% poor solvent, the DLS analyses revealed a mean hydrodynamic diameter of 121.5–143.2 nm for the particles that form the sample (Fig. S11, ESI†). In contrast, no detectable peak was found for the $CHCl_3$ solution of **5**, since **5** was in the molecular well-dissolved state.[27] The emission spectra for the lyophilized aggregates were also measured (black dotted lines in Fig. 2a and Fig. S6a, ESI†).

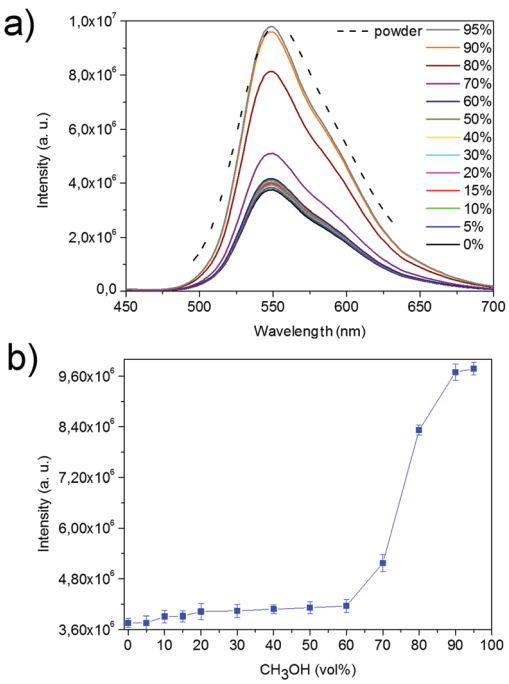

Fig. 2 (a) Emission spectra of **5** (λ_{ex} = 360 nm) measured in different $CHCl_3$–CH_3OH compositions; (b) changes in the emission intensity (λ_{em} = 548 nm) for the samples with different vol% of poor solvent (CH_3OH). For (a), the annotation stands for the volumetric ratio of CH_3OH in each mixture. The black dotted lines in (a) indicate the emission spectrum for the lyophilized aggregates. For (b), error bars are also shown. The concentration of the samples is 2×10^{-5} M.

The spectra of the lyophilized aggregates from the $CHCl_3$–hexane or $CHCl_3$–CH_3OH mixtures (95 vol% poor solvent) were very similar and indicate that the poor solvent type has no significant influence on the AIEE behaviour of **5**. It is worth noting that the photoluminescence (PL) experiments were repeated three times to check the reproducibility of the results.

Having photophysically characterized **5**, we began to study its application in caesium cation (Cs^+) recognition. We hypothesized that the addition of Cs^+ to the aggregates of **5** in the $CHCl_3$–CH_3OH solvent system might cause disaggregation of **5**, leading to a drop in fluorescence intensity[28] (see Fig. 3 for a graphical representation of the proposed process).

The recognition properties of **5** were examined at room temperature by recording emission spectra (λ_{ex} = 360 nm) in $CHCl_3$–CH_3OH mixtures with 95 vol% poor solvent in which the concentration of **5** was 2×10^{-5} M and the amount of Cs^+ was increased gradually from 0.0 equiv. to 25.0 equiv. These recognition experiments were repeated three times. Upon the addition of Cs^+ (in the form of $CsNO_3$[29]), a significant drop in the fluorescence intensity was observed (Fig. 4a). This feature could be ascribed to the disaggregation of **5**. A change in the emission intensity was found between the samples. In fact, this behaviour was constant over 2 equiv. of Cs^+ (Fig. S8, ESI†). More importantly, it can be claimed that the designed method can be used for the quantification of Cs^+ in solution. The response to Cs^+ fit well with the logarithmic relationship (coefficient of determination (R^2) equal to 0.98; Fig. S8, ESI†). This logarithmic fit suggests that the studied interaction might follow a cooperative model in which the binding of one analyte molecule increases the ability of the receptor to bind another analyte molecule.[30,31] This cooperative mechanism model is likely to be associated with an increase in the steric availability of concave sites in the sumanene units of **5**, as well as the flexibility of aggregated **5** after the formation of the first Cs^+ complex.

To obtain an insight into the stoichiometry of the formed systems, Job's plot analysis was performed (Fig. S12, ESI†). This revealed that the **5**: Cs^+ complex stoichiometry was 1 : 2. Due to our previous studies on the interactions between Cs^+ and sumanene derivatives in their neutral state,[15,16] this finding suggests that the driving force of the observed disaggregation behaviour was indeed the formation of the sandwich complex between Cs^+ and two sumanene molecules. To confirm this further, cold spray ESI-MS analysis was performed with a mixture comprising compound **5** and 25 equiv. of Cs^+ (Fig. 4c). The ESI-MS analysis confirmed the formation of the sandwich complex, as the peak originating from the presence of this system (*ca.* 2619 *m*/*z*) was clearly detected.

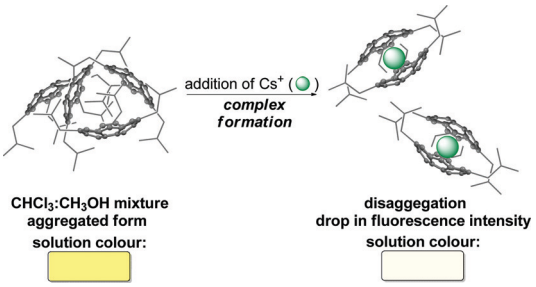

Fig. 3 Graphical representation of the proposed recognition process.

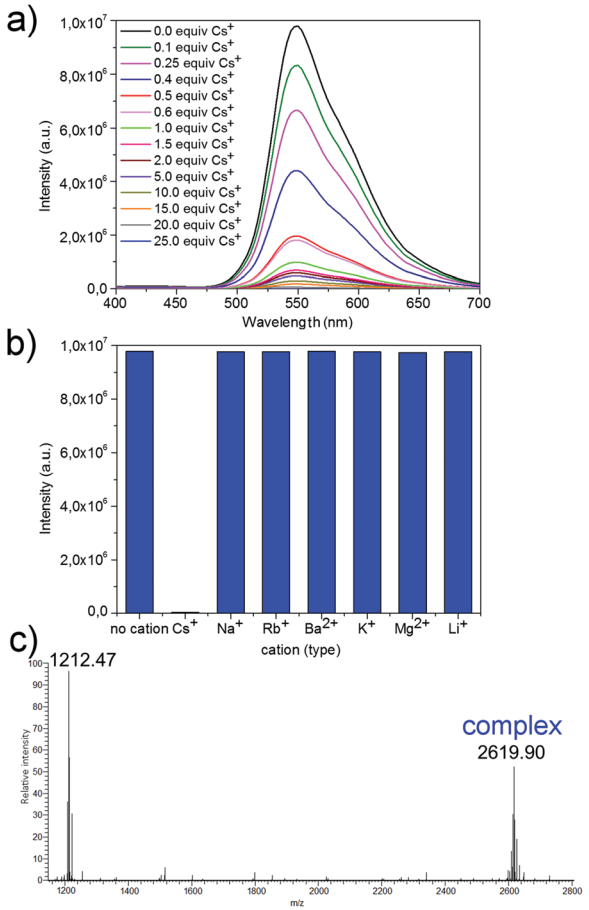

Fig. 4 (a) Emission spectra of aggregated **5** (λ_{ex} = 360 nm) in the presence of a molar equiv. of Cs^+; (b) emission intensity (λ_{em} = 548 nm) changes of aggregated **5** upon the addition of different metal cations (25 equiv.); (c) cold spray ESI-MS spectrum of **5** in the presence of 25 equiv. of Cs^+ (the *m*/*z* peak originating from the presence of the sandwich complex is marked). For (b), error bars are also shown. The concentration of the samples is 2×10^{-5} M.

To investigate the specificity of Cs^+ recognition, emission spectra (λ_{ex} = 360 nm) were measured in the presence of an excess (25 equiv.) of other metal cations (in the form of metal nitrates). A significant drop in the emission intensity was found only upon the addition of Cs^+ (Fig. 4b). In practice, no changes were observed for the samples containing cations of other metals. This means that the recognition property of **5** is highly Cs^+-specific. Additionally, the Cs^+ recognition process was found to be selective, as no differences in the emission intensities between the samples after treatment with Cs^+ alone or with Cs^+ in the presence of cations of other metals were found (Section S7, ESI†).

Time-course emission spectra (λ_{ex} = 360 nm) were measured in a $CHCl_3$–CH_3OH mixture with 95 vol% poor solvent in the presence of 2 equiv. of Cs^+ (Fig. S9, ESI†). A significant drop in the emission intensity was observed rapidly, within just 15 sec (a similar trend was also observed for 25 equiv. of Cs^+, as shown

Table 1 LOD values for various Cs^+ recognition materials

Material	LOD [μM]	Ref.
Compound **5**	0.15	This work
Various sumanenylferrocenes	12–70	15
Tris(ferrocenylmethidene)sumanene	0.02	16
Various calixarenes	0.096–0.770	35*a*,*b*
Squaraine	0.096	35*c*
Boron-dipyrromethene (BODIPY)	0.273	35*d*

in Fig. S10, ESI†). No significant changes in the emission intensity were found after 1 min. In the case of the addition of 25 equiv. of Cs^+ (Fig. S10, ESI†), no strong intensity was observed within 1 min. This means that the reported Cs^+ recognition is characterized by a very short response time.

Previously reported sumanene-containing electrochemical sensors exhibited reversible binding of Cs^+.[15,16] To check whether the disaggregation-based methodology described herein is characterized by a similar reversible behaviour, aggregated **5** – after treatment with Cs^+ – was thoroughly washed with the $CHCl_3$–CH_3OH mixture and emission spectra were then measured in the presence or absence of Cs^+ (see full experimental data in Section S8 of the ESI†). The outcomes of these experiments were highly consistent with that from the first treatment of aggregated **5** with Cs^+, and this means that Cs^+ binding by **5** is reversible. Finally, to obtain an insight into the binding parameters, the association constant (K_a) and limit of detection (LOD) values were determined. K_a was estimated using the Benesi–Hildebrand equation[32,33] (see details in Section S9 of the ESI†) and was equal to 9.0×10^5 M^{-2}, whilst the LOD value[34] was found to be equal to 1.5×10^{-7} M. The LOD value is comparable with the values for other Cs^+ recognition materials (Table 1), including sumanene-tethered receptors. Importantly, compound **5** exhibited a very satisfactory LOD value amongst those of the fluorescent receptors listed in Table 1 (excluding tris(ferrocenylmethidene)sumanene, which is an electrochemical sensor).

In conclusion, we have demonstrated that a novel sumanene derivative, **5**, shows strong yellow light emission and is an AIEE-active compound. These findings gave rise to the preparation of a highly sensitive turn-off fluorescent probe, which is dedicated to very specific and selective Cs^+ detection that was characterized by a fast response. All these beneficial features prove that **5** is a highly attractive molecule from a design point of view of recognition materials for caesium-contaminated probes. Our future work in this topic will include the preparation of other sumanene-containing fluorophores that might exhibit aggregation-induced effects, as well as the examination of their application potential with a focus on Cs^+ detection.

Financial support from Warsaw University of Technology and JSPS KAKENHI (JP19H00912) are acknowledged.

Conflicts of interest

There are no conflicts to declare.

Notes and references

1 H. Sakurai, T. Daiko and T. Hirao, *Science*, 2003, **301**, 1878.
2 T. Amaya and T. Hirao, *Chem. Commun.*, 2011, **47**, 10524.
3 E. Nestoros and M. C. Stuparu, *Chem. Commun.*, 2018, **54**, 6503.
4 T. Amaya and T. Hirao, *Chem. Rec.*, 2015, **15**, 310.
5 M. Saito, H. Shinokubo and H. Sakurai, *Mater. Chem. Front.*, 2018, **2**, 635.
6 S. Alvi and R. Ali, *Beilstein J. Org. Chem.*, 2020, **16**, 2212.
7 S. H. Mahadevegowda and M. C. Stuparu, *Eur. J. Org. Chem.*, 2017, 570.
8 I. Hisaki, H. Toda, H. Sato, N. Tohnai and H. Sakurai, *Angew. Chem., Int. Ed.*, 2017, **56**, 15294.
9 Y. Yakiyama, T. Hasegawa and H. Sakurai, *J. Am. Chem. Soc.*, 2019, **141**, 18099.
10 B. Topolinski, B. M. Schmidt, S. Higashibayashi, H. Sakurai and D. Lentz, *Dalton Trans.*, 2013, **42**, 13809.
11 T. Amaya, S. Katoh, T. Moriuchi and T. Hirao, *Org. Chem. Front.*, 2019, **6**, 1032.
12 H. Sakane, T. Amaya, T. Moriuchi and T. Hirao, *Angew. Chem., Int. Ed.*, 2009, **48**, 1640.
13 T. Amaya, W.-Z. Wang, H. Sakane, T. Moriuchi and T. Hirao, *Angew. Chem., Int. Ed.*, 2010, **49**, 403.
14 S. N. Spisak, Z. Wei, A. Y. Rogachev, T. Amaya, T. Hirao and M. A. Petrukhina, *Angew. Chem., Int. Ed.*, 2017, **56**, 2582.
15 A. Kasprzak and H. Sakurai, *Dalton Trans.*, 2019, **48**, 17147.
16 A. Kasprzak, A. Kowalczyk, A. Jagielska, B. Wagner, A. M. Nowicka and H. Sakurai, *Dalton Trans.*, 2020, **49**, 9965.
17 U. D. Priyakumar, M. G. P. Krishna and G. N. Sastry, *Tetrahedron Lett.*, 2004, **60**, 3037.
18 D. Vijay, H. Sakurai, V. Subramanian and G. N. Sastry, *Phys. Chem. Chem. Phys.*, 2012, **14**, 3057.
19 U. D. Priyakumar and G. N. Sastry, *Tetrahedron Lett.*, 2003, **44**, 6043.
20 T. J. Yasunari, A. Stohl, R. S. Hayano, J. F. Burkhart, S. Eckhardt and T. Yasunari, *Proc. Natl. Acad. Sci. U. S. A.*, 2011, **108**, 19530.
21 Y. Masumoto, Y. Miyazawa, D. Tsumune, T. Tsubono, T. Kobayashi, H. Kawamura, C. Estournel, P. Marsaleix, L. Lanerolle, A. Mehra and Z. D. Garraffo, *Elements*, 2012, **8**, 207.
22 H. Kaeriyama, *Fish. Oceanogr.*, 2017, **26**, 99.
23 T. Amaya, K. Mori, H.-L. Wu, S. Ishida, J.-I. Nakamura, K. Murata and T. Hirao, *Chem. Commun.*, 2007, 1902.
24 J. Mei, N. L. C. Leung, R. T. K. Kwok, J. W. Y. Lam and B. Z. Tang, *Chem. Rev.*, 2015, **115**, 11718.
25 Y. Hong, J. W. Y. Lam and B. Z. Tang, *Chem. Soc. Rev.*, 2011, **40**, 5361.
26 P. Kaewmati, Y. Yakiyama, H. Ohtsu, M. Kawano, S. Haesuwannakij, S. Higashibayashi and H. Sakurai, *Mater. Chem. Front.*, 2018, **2**, 514.
27 T. S. Reddy, J. Hwang and M.-S. Choi, *Dyes Pigm.*, 2018, **158**, 412.
28 N. H. Kim, M. Won, J. S. Kimb, Y. Huh and D. Kim, *Dyes Pigm.*, 2019, **160**, 647.
29 The type of counter-anion might influence of Cs+ binding ability, see e.g., X.-F. Chen, Q. Ma, Z. Wang, Z. Xie, Y. Song, Y. Ma, Z. Yang and X. Zhao, *Chem. – Asian J.*, 2020, **15**, 4104. Herein, no significant differences in the behavior between $CsNO_3$ and CsCl were found.
30 L. K. S. von Krbek, C. A. Schalley and P. Thordarson, *Chem. Soc. Rev.*, 2017, **46**, 2622.
31 J. Gómez-Vega, R. A. Moreno-Corral, H. S. Ortega, D. O. Corona-Martínez, H. Höpfl, R. R. Sotelo-Mundo, A. Ochoa-Terán, R. E. Escobar-Picos, J. Z. Ramírez-Ramírez, O. Juárez-Sánchez and K. O. Lara, *Supramol. Chem.*, 2019, **31**, 322.
32 S. Goswami, K. Aich, S. Das, A. K. Das, A. Manna and S. Halder, *Analyst*, 2013, **138**, 1903.
33 H. A. Benesi and J. H. Hildebrand, *J. Am. Chem. Soc.*, 1949, **71**, 2703.
34 LOD was calculated using the following equation: $LOD = 3S_a/b$, where s_a stands for the standard deviation of the y-intercept and b is the slope of the calibration curve.
35 (*a*) N. Kumar, Q. Pham-Xuan, A. Depauw, M. Hemadi, N.-T. Ha-Duong, J.-P. Lefevre, M.-H. Ha-Thi and I. Leray, *New J. Chem.*, 2017, **41**, 7162; (*b*) V. Souchon, I. Leray and B. Valeur, *Chem. Commun.*, 2006, 4224; (*c*) B. Radaram, T. Mako and M. Levine, *Dalton Trans.*, 2013, **42**, 16276; (*d*) E. Özcan and B. Çoşut, *ChemistrySelect*, 2018, **3**, 7940.

